Headline Articles

Oscillations of Membrane Current or Membrane Potential and Voltammetric Elucidation of Their Mechanisms

Kohji Maeda, Wataru Hyogo, Shuzo Nagami, and Sorin Kihara*

Department of Chemistry, Kyoto Institute of Technology, Matsugasaki, Sakyo-ku, Kyoto 606

(Received January 13, 1997)

Novel oscillations of membrane current or membrane potential were observed when the transfer of Na^+ from one aqueous solution (W1) containing 0.1 M NaCl to another (W2) in the absence of Na^+ through a liquid membrane (LM) containing dilute Na^+ was forced by an applied membrane potential or membrane current, respectively. The current oscillation was induced by the addition of acetylcholine in W1, and inhibited by the addition of such hydrophobic ions as tetraalkylammonium ions or glutamate ion in W1. These oscillations were similar to those at biomembranes with so-called "sodium channels" as regards both induction and inhibition, though the liquid membrane system did not contain any channel proteins. The current and potential oscillations were also inhibited by the addition of bovine serum albumin in W2. The mechanisms of the oscillations, the induction and the inhibitions were elucidated by referring to voltammograms for the ion transfer through a membrane as well as those at aqueous/membrane interfaces, and by taking into account the adsorption of Na^+ at the LM/W2 interface. Various LM systems which exhibit the oscillations accompanied by transports of ions other than Na^+ were also investigated, and the general feature of the oscillations of membrane current or potential is discussed.

The oscillation of membrane current or potential accompanied by an ion transfer through a membrane, which is closely related to the electrical excitability in living organisms,[1] has been investigated extensively by many authors using biomembranes or artificial membranes.[2,3] Also, many efforts have been made to develop new sensors utilizing the oscillations because of the high sensitivity and selectivity of the oscillations.[4,5]

Most of the oscillations observed with biomembranes have been attributed to the gating of the "ion channel" composed of transmembrane proteins present in biomembranes, and tremendous efforts have been made to elucidate the gating process, mainly by reconstitution of channel proteins into bilayer membranes.[6—8]

On the other hand, the oscillations have also been observed with thick liquid membranes as well as artificial bilayer lipid membranes, *BLM*, in the absence of the channel protein, and these oscillations are expected to offer plenty of fundamental information useful in elucidating the oscillation processes at biomembranes in living organisms.[2,3]

Since even the non-channel oscillations at liquid membranes and artificial *BLM* are revealed by way of the tangle of plural ion transfer reactions and interfacial adsorptions, though their generating processes are supposed to be much simpler than those at biomembranes, new methodologies and concepts are required for further understanding of oscillation processes and physiological phenomena relative to the oscillations.

In the previous proceedings[9] and review,[3] the authors briefly introduced novel types of oscillations of membrane current or membrane potential observed during the transport of Na^+ from one aqueous solution to another through a liquid membrane, and proposed the corresponding mechanisms of the oscillations based on the voltammetric concept as well as the voltammogram for ion transfer through a membrane, *VITTM*, and the voltammogram for ion transfer at the aqueous/membrane interface, *VITAMI*. Here, *VITAMI* is the same method of the voltammetry for the ion transfer at an interface of two immiscible electrolyte solutions, *VITIES*,[10—13] which has been recognized as one of the promising methods for understanding both the static and dynamic features of the ion transfer at a liquid/liquid or liquid/membrane interface. The adsorption at the interface taking part in the oscillation can also be investigated by the *VITIES* since it causes the voltammetric maximum.[14,15] The induction and inhibition of the oscillation of the membrane current were also investigated. The current oscillation was found to have characteristics similar to those of the oscillation at biomembrane with the so-called "sodium channel", though the membrane system did not contain any channel proteins.

In the present paper, the details of the oscillations of the membrane current and potential observed with the transport

of Na^+ are described, and mechanisms for the oscillations, the induction and the inhibition are discussed. The general condition to observe the oscillations are also discussed, with reference to results on other oscillations which have been found so far in the author's laboratory.

Experimental

Electrochemical Measurements. A glass cell, illustrated in Fig. 1, was used for the observation of the oscillations of the membrane current (current between W1 and W2, I_{W1-W2}) and the membrane potential (potential difference between W1 and W2, ΔV_{W1-W2}), *VITTM* and *VITAMI*. Two aqueous phases, W1 and W2 (2.0 ml each), were separated by 1.0 ml of a nitrobenzene, NB, which worked as a liquid membrane, LM, with an interfacial area of 1.0 cm^2 and thickness of 1.0 cm.

An example of the cell configuration is given in Eq. 1.

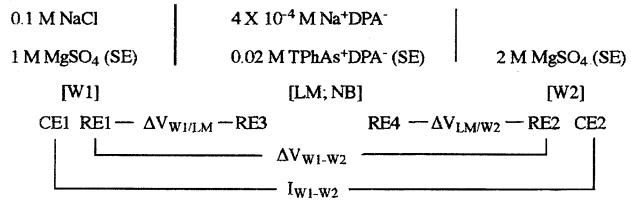

(1)

Here SE denotes the supporting electrolyte. DPA^- and $TPhAs^+$ mean dipicrylaminate and tetraphenylarsonium ions, respectively. The concentrations of SE ($MgSO_4$) in W1 and W2 were made to be 1 M and 2 M, respectively, in order to stabilize the LM between W1 and W2 with the aid of the difference in specific gravities. W2 was stirred at about 200 rpm when oscillations were investigated.

The ΔV_{W1-W2} was applied with the aid of two silver/silver chloride electrodes, RE1 and RE2, as the potential of RE2 vs. RE1 in order to realize the ion transfer between W1 and W2 through the LM. The I_{W1-W2} due to the ion transfer was detected by using two platinum wire electrodes, CE1 and CE2. Two $TPhAs^+$ ion selective electrodes (TPhAsE) with the configuration shown in Eq. 2, RE3 and RE4, were set in LM close to the W1/LM and LM/W2 interfaces, respectively, and the potential differences at the W1/LM and LM/W2 interfaces, $\Delta V_{W1/LM}$ and $\Delta V_{LM/W2}$, during the ion transfer were monitored as potentials of RE3 vs. RE1 and RE2 vs. RE4, respectively.

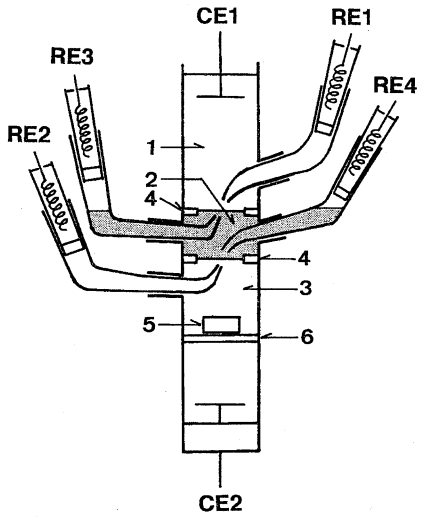

Fig. 1. Glass cell employed to observe the oscillation and the ion transfer voltammogram. 1; aqueous phase (W1). 2; organic liquid membrane (LM). 3; aqueous phase (W2). 4; polytetrafluoroethylene ring. 5; stirring bar. 6; glass filter. RE1, RE2, RE3, and RE4; reference electrodes. CE1 and CE2; counter electrodes.

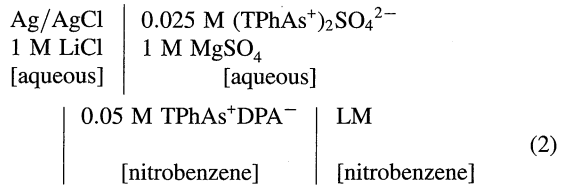

(2)

The *VITTM* was recorded by scanning ΔV_{W1-W2} and detecting I_{W1-W2}. The *VITAMI* was obtained by monitoring the variation of $\Delta V_{W1/LM}$ or $\Delta V_{LM/W2}$ as a function of I_{W1-W2}.

The polarogram for ion transfer at the interface between an aqueous phase, W, and NB was investigated at the electrolyte solution dropping electrode using a polarographic cell described previously.[16,17] The potential difference at the W/NB interface was applied as the potential of a silver/silver chloride electrode in W vs. TPhAsE or TPhBE in NB. Here, TPhBE denotes a tetraphenylborate ion ($TPhB^-$) selective electrode, of which the configuration was given elsewhere.[17,18] The electrolyte solution dropping electrode was also used for the measurement of the drop time–potential curve.

Conductances of electrolyte solutions were measured to evaluate association constants of ion pairs according to previous works.[14,19]

All electrochemical measurements were carried out at 25±0.5 °C.

Apparatus. The potentiostat/galvanostat, function generator, *X–t* and *X–Y* recorders used were identical with those mentioned in previous papers.[14,20]

Chemicals. In order to prepare $TPhAs^+DPA^-$, a methanol solution of $TPhAs^+Cl^-$ (Aldrich) was mixed with a methanol solution of Na^+DPA^- (Tokyo Kasei Kogyo). After filtration, the precipitate of $TPhAs^+DPA^-$ was dissolved with acetonitrile and then recrystallized by adding water to the acetonitrile solution. The recrystallization was repeated three times. Similar procedures were adopted to prepare DPA^- salts of K^+, tetrapropylammonium ($TPrA^+$) and tetrabutylammonium (TBA^+) ions. Tetrahexylammonium ion ($THexA^+$) salt of $TPhB^-$ was prepared by mixing $THexA^+Br^-$ with Na^+TPhB^- in water, and the precipitate was recrystallized from an acetone-ethanol mixture. $TPhB^-$ salt of Cs^+, tetramethylammonium ion (TMA^+) or $TPrA^+$ and tetrapentylammonium ($TPenA^+$) salt of SO_4^{2-} were prepared and recrystallized according to the procedures described previously.[14,21] Bovin serum albumin (BSA) used was a product of Wako (Lot. LEP 3277). Nitrobenzene which had been passed through a column of activated alumina and then distilled under reduced pressure (mp: 5.67 °C, bp: 210.8 °C) was shaken with water prior to use for the electrochemical measurements.

All other reagents were of reagent grade and were used without further purification.

Results and Discussion

1. Oscillation of Membrane Current under an Applied Membrane Potential. Curve 1 in Fig. 2 gives an example of the oscillation of membrane current observed with the cell of Eq. 1 by applying a constant ΔV_{W1-W2} of −0.48 V and measuring the time course of I_{W1-W2}. The oscillation lasted for more than 2 h. Curves 2 and 3 show time courses of

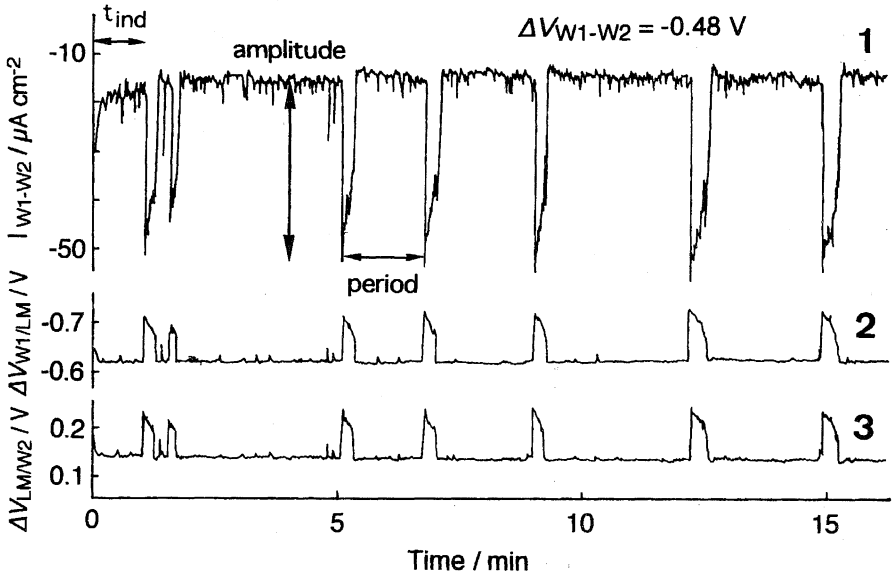

Fig. 2. Time courses of membrane current (curve 1) and the potential differences at the W1/LM interface (curve 2) and LM/W2 interface (curve 3) observed by applying a membrane potential of −0.48 V to the cell of Eq. 1.

$\Delta V_{W1/LM}$ and $\Delta V_{LM/W2}$ observed simultaneously with curve 1. From these curves, it is obvious that the current oscillation is accompanied by the oscillations of $\Delta V_{W1/LM}$ and $\Delta V_{LM/W2}$, though the amplitudes are not large (about 0.08 V). Here, it is notable that the amplitude of the oscillation of $\Delta V_{W1/LM}$ is the same as that of $\Delta V_{LM/W2}$.

The range of applied ΔV_{W1-W2} available for the current oscillation was between −0.40 and −0.55 V. When ΔV_{W1-W2} was more negative in the range, the amplitude of the oscillation was larger and the period was longer as follows; Amplitudes (average of 100 oscillations in 5 measurements) were 53, 38 or 22 μA cm^{-2} and periods (average of 100 oscillations in 5 measurements) were 2.1, 1.8 or 1.6 min when ΔV_{W1-W2} were −0.53, −0.48 or −0.43 V, respectively. The time required to induce the oscillation, t_{ind}, was not reproducible and was from 30 s to 3 min at any ΔV_{W1-W2} between −0.40 and −0.55 V.

The oscillation at ΔV_{W1-W2}=−0.48 V was not observed within 2 h when the concentration of Na^+DPA^- was less than 10^{-4} M or more than 2×10^{-3} M (the concentration of $TPhAs^+DPA^-$: 0.02 M, 1 M=1 mol dm^{-3}), and when the concentration of $TPhAs^+DPA^-$ was less than 0.01 M or more than 0.07 M (the concentration of Na^+DPA^-: 4×10^{-4} M). The characteristics of the oscillation observed by varying concentrations of Na^+DPA^- or $TPhAs^+DPA^-$ are summarized in Table 1. In the table, activities of dissociated Na^+ and associated Na^+ with DPA^-, Na^+DPA^-, in LM (NB) calculated based on ion-pair formation constants, K_{ip}, in NB are added. Here, K_{ip} of Na^+DPA^- and $TPhAs^+DPA^-$ in NB were assumed to be 230 and 480, respectively, though K_{ip} determined by conductivity measurements with the aid of the Shedlovsky method[22] were not very reproducible and were 230±80 and 480±120.

It is obvious from Table 1 that the amplitude of the current oscillation strongly depends on the activity of the dissociated Na^+, but hardly on the activity of the ion pair, Na^+DPA^-.

2. Induction or Inhibition of the Current Oscillation. Similarly to the induction or the inhibition of the current oscillation at a biomembrane with a "sodium channel", the current oscillation at the liquid membrane (without any channel proteins) accompanied by the transfer of Na^+ can be induced by acetylcholine ion (Ach^+) or inhibited by such rather hydrophobic ions as alkylammonium and glutamate ions.

The current oscillation shown in Fig. 3 was induced by adding 2×10^{-4} M Ach^+ into W1 of the membrane system as Eq. 1, to which ΔV_{W1-W2} of −0.30 V had been applied instead of −0.48 V. Here, −0.30 V is not the ΔV_{W1-W2} value effective for the oscillation in the absence of Ach^+. The life time of the induced current oscillation was much shorter than that observed by applying −0.48 V to the system in the absence of Ach^+, and was from 20 to 40 min. The concentration range of Ach^+ effective for the induction was from 7×10^{-5} to 3×10^{-4} M. The life time was longer with higher concentration of Ach^+ as follows: 5 to 15, 10 to 25, 20 to 40, and 30 to 45 min when concentrations were 7×10^{-5}, 1.2×10^{-4}, 2×10^{-4}, and 3×10^{-4} M, respectively. The amplitude was larger with higher concentration of Ach^+ as follows: about 25, 33, 45 or 50 μA cm^{-2} when concentrations were 7×10^{-5}, 1.2×10^{-4}, 2×10^{-4} or 3×10^{-4} M, respectively. Periods observed were not very reproducible especially when the concentration of Ach^+ was as low as 7×10^{-5} or 1.2×10^{-4} M.

The current oscillation observed by applying ΔV_{W1-W2}= −0.48 V was inhibited when one of the rather hydrophobic ions such as tetraethylammonium ion (TEA^+), TBA^+ or glutamate ion was added to W1 to a final concentration of more than 10^{-3} M or when more than 10^{-6} M of BSA was added to W2.

3. The Oscillation of Membrane Potential under an Applied Membrane Current. When a constant I_{W1-W2} of −20 μA cm^{-2} was applied to the membrane system of Eq. 1 in order to realize the transfer of Na^+ from W1 to W2

Table 1. Dependence of Characteristics of Oscillations of Membrane Current and Membrane Potential on Concentrations of Na^+DPA^- and $TPhAs^+DPA^-$

Oscillation of membrane current: The results obtained by applying a membrane potential (ΔV_{W1-W2}) of −0.48 V. The amplitude and period are averages of 100 oscillations in 5 measurements, and induction time (t_{ind}) is the result of 5 measurements. Oscillation of membrane potential: The results obtained by applying a membrane current (I_{W1-W2}) of $-20\ \mu A\ cm^{-2}$. The amplitude and period are averages of 50 oscillations in 5 measurements, and induction time (t_{ind}) is the average of 5 measurements.

Concentration of Na^+DPA^-	Concentration of $TPhAs^+DPA^-$	Activity of Na^+	Activity of Na^+DPA^-	Oscillation of membrane current			Oscillation of membrane potential		
				Amplitude	Period	t_{ind}[a]	Amplitude	Period	t_{ind}
$\times 10^{-4}$ M	M	$\times 10^{-4}$ M	$\times 10^{-4}$ M	$\mu A\ cm^{-2}$	min	min	V	min	min
5.03	0.01	2.5	2.0	47	1.7	—	0.47	1.8	1.7
4.06	0.02	1.7	2.0	38	1.8	—	0.48	1.2	1.4
3.66	0.03	1.3	2.0	27	1.8	—	0.47	0.5	0.7
3.43	0.04	1.1	2.0	20	2.1	—	0.45	0.3	0.4
3.27	0.05	1.0	2.0	13	2.1	—	—[b]	—[b]	—[b]
3.16	0.06	0.9	2.0	8	2.2	—	—[b]	—[b]	—[b]
3.21	0.01	1.6	1.3	35	1.5	—	0.47	1.0	1.5
3.94	0.02	1.6	1.9	37	1.8	—	0.46	1.2	1.3
4.51	0.03	1.6	2.5	38	1.7	—	0.48	1.1	1.3
4.97	0.04	1.6	2.9	37	1.9	—	0.49	1.2	1.4
5.39	0.05	1.6	3.4	39	1.8	—	0.48	1.1	1.5
5.75	0.06	1.6	3.6	40	1.7	—	0.47	1.0	1.2

a) t_{ind} of current oscillations were not reproducible, and distributed between 0.5 and 5 min. b) The potential oscillation was not observed under the applied membrane current of $-20\ \mu A\ cm^{-2}$.

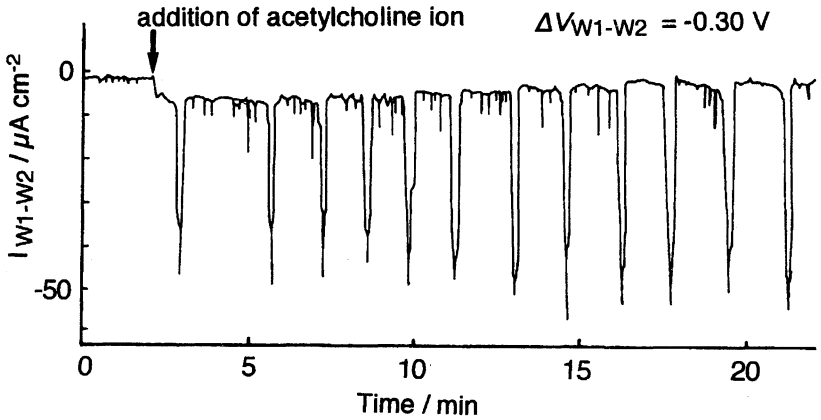

Fig. 3. The induction of the oscillation of membrane current by the addition of 2×10^{-4} M acetylcholine ion in W1 of the cell of Eq. 1 to which a membrane potential of −0.30 V has been applied.

through LM, and the time course of ΔV_{W1-W2} was investigated, the oscillation of ΔV_{W1-W2} between about −0.4 and −0.9 V was observed as illustrated in curve 1 of Fig. 4. The oscillation continued for 1 to 2 h. Curves 2 and 3 are time courses of $\Delta V_{W1/LM}$ and $\Delta V_{LM/W2}$ observed simultaneously with curve 1. It was found that the pattern of the oscillation of ΔV_{W1-W2} coincided almost completely with that of $\Delta V_{LM/W2}$, whereas the oscillation of $\Delta V_{W1/LM}$ was negligible. Hence, the oscillation of ΔV_{W1-W2} was attributed to that of $\Delta V_{LM/W2}$.

The range of I_{W1-W2} effective for the oscillation with the cell of Eq. 1 was between −15 and $-40\ \mu A\ cm^{-2}$. Though the amplitude of the oscillation was almost indifferent to the magnitude of the applied I_{W1-W2}, the period and t_{ind} lengthened with the decrease of I_{W1-W2} as follows; Periods (average of 50 oscillations in 5 measurements) were 1.2, 0.8 or 0.5 min and t_{ind} (average of 5 measurements) were 1.4, 1.1 or 0.7 min when I_{W1-W2} were −20, −30 or $-40\ \mu A\ cm^{-2}$, respectively.

The oscillation was not observed at any I_{W1-W2} when the concentration of Na^+DPA^- was less than 10^{-4} M or more than 2×10^{-3} M (the concentration of $TPhAs^+DPA^-$: 0.02 M), and when the concentration of $TPhAs^+DPA^-$ was less than 0.01 M or more than 0.07 M (the concentration of Na^+DPA^-: 4×10^{-4} M). The characteristics of the potential oscillation observed by varying concentrations of Na^+DPA^- or $TPhAs^+DPA^-$ are summarized in Table 1. It is obvious from the table that the amplitude of the potential oscillation is practically independent of both activities of the dissociated Na^+ and the ion pair, Na^+DPA^-, but period and t_{ind} depend strongly on the activity of the dissociated Na^+.

When SE in LM, $TPhAs^+DPA^-$, in the system of Eq. 1

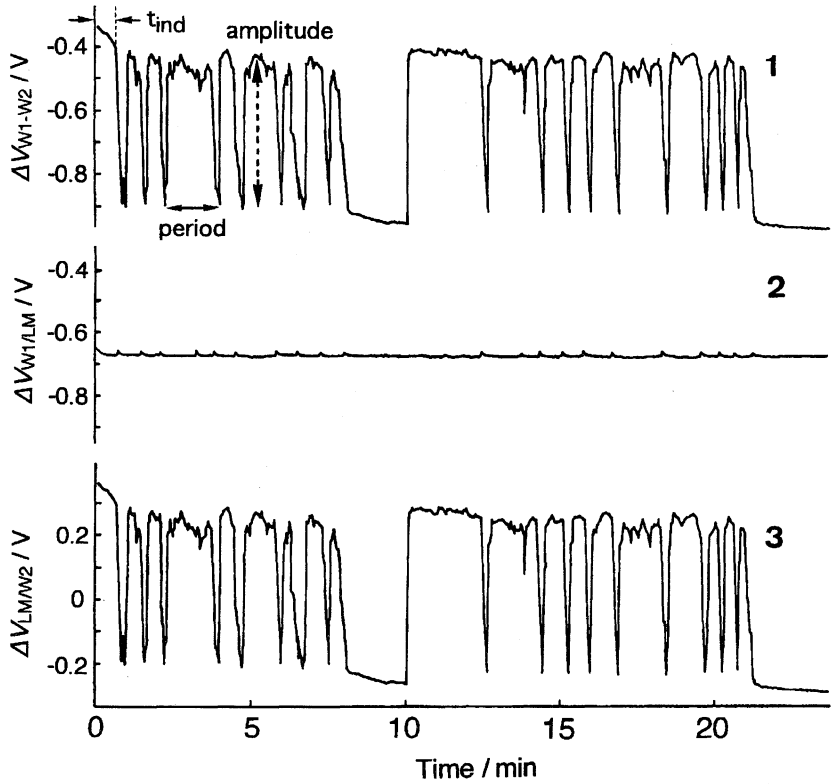

Fig. 4. Time courses of ΔV_{W1-W2} (curve 1), $\Delta V_{W1/LM}$ (curve 2), and $\Delta V_{LM/W2}$ (curve 3) observed by applying a membrane current of -20 μA cm^{-2} to the cell of Eq. 1.

was replaced by TBA^+DPA^- or $TPrA^+DPA^-$, the positive limit of ΔV_{W1-W2} in the oscillation was almost unchanged though the negative limit of ΔV_{W1-W2} became about 0.10 or 0.17 V, respectively, less negative, and hence the amplitude decreased in a similar manner.

The potential oscillation observed by applying $I_{W1-W2} = -20$, -30 or -40 μA cm^{-2} to the cell of Eq. 1 disappeared when more than 10^{-6} M of BSA was added to W2.

4. Voltammograms for the Ion Transfer through LM, *VITTM*, and at Interfaces of W1/LM and LM/W2, *VITAMI*. The *VITTM* and *VITAMI* were investigated in order to understand the processes involved in the oscillations.

Curve 1 in Fig. 5 is the *VITTM* recorded with the cell of Eq. 1 by scanning ΔV_{W1-W2} and measuring I_{W1-W2}. Curves 2 and 3 are *VITAMIs* at W1/LM and LM/W2 interfaces recorded simultaneously with curve 1, measuring $\Delta V_{W1/LM}$ and $\Delta V_{LM/W2}$ as the function of I_{W1-W2}

An extremely large current peak appeared in voltammograms 1 and 3. The peak current was about 12 times larger than the ordinary diffusion-controlled current for the transfer of Na^+ from NB containing 4×10^{-4} M Na^+ to W. Consulting with voltammograms at the W/NB interface recorded under various conditions, the negative current peak in voltammogram 3 was attributed to the maximum due to the transfer of Na^+ from LM to W2 enhanced by interfacial adsorption (which will be discussed later). The final rise and the final descent in voltammogram 2 or 3 were confirmed to be due to transfers of $TPhAs^+$ from LM to W1 and Na^+ from W1 to LM or DPA^- from LM to W2 and $TPhAs^+$ from LM to W2, respectively.

In the previous paper[20] on the ion transport through a membrane, it was demonstrated that the relation among ΔV_{W1-W2} in curve 1, $\Delta V_{W1/LM}$ in curve 2 and $\Delta V_{LM/W2}$ in curve 3 at a definite I_{W1-W2} value can be approximated by Eq. 3, when W1, W2, and LM contain sufficient concentrations of ions as in the case of Eq. 1.

$$\Delta V_{W1-W2} = \Delta V_{W1/LM} + \Delta V_{LM/W2}. \quad (3)$$

This equation suggests that the membrane potential in the presence of sufficient electrolytes in W1, W2, and LM is primarily determined by the potential differences at the two interfaces, which depend on ion transfer reactions at the interfaces.

Taking into account the relation of Eq. 3, the negative current peak in voltammogram 1 in Fig. 5 is considered to be composed of the peak in voltammogram 3 due to the enhanced transfer of Na^+ from LM to W2 and the final descent in voltammogram 2 due to the transfer of Na^+ from W1 to LM.

The maximum peaks in voltammograms 1 and 3 in Fig. 5 were not observed when the concentration of Na^+DPA^- was less than 10^{-4} M (the concentration of $TPhAs^+DPA^-$: 0.02 M). Figure 6 shows the dependence of the maximum peak on the activity of the dissociated Na^+, a_{Na^+}, or on that of the associated Na^+, $a_{Na^+DPA^-}$, under the condition that $a_{Na^+DPA^-}$ or a_{Na^+} was constant, respectively. The magnitude of the maximum peak depended strongly on a_{Na^+}, although the maxi-

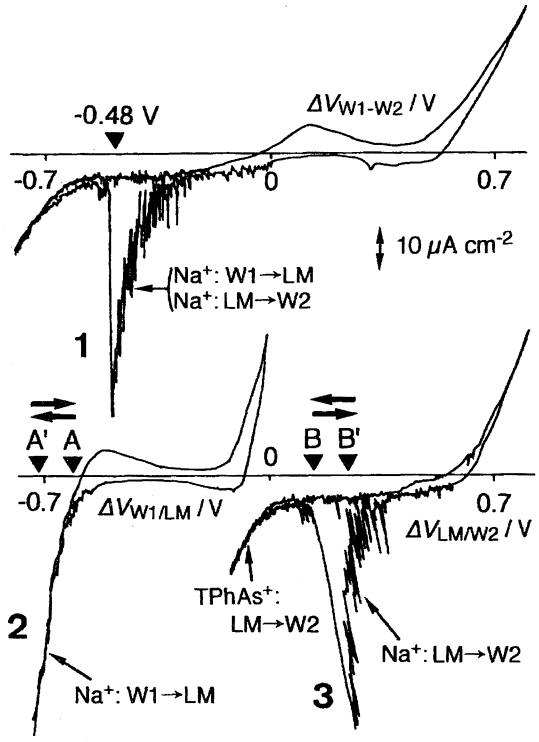

Fig. 5. Voltammograms for ion transfer through a membrane (curve 1), at the W1/LM interface (curve 2), and at the LM/W2 interface (curve 3) recorded with the cell of Eq. 1.

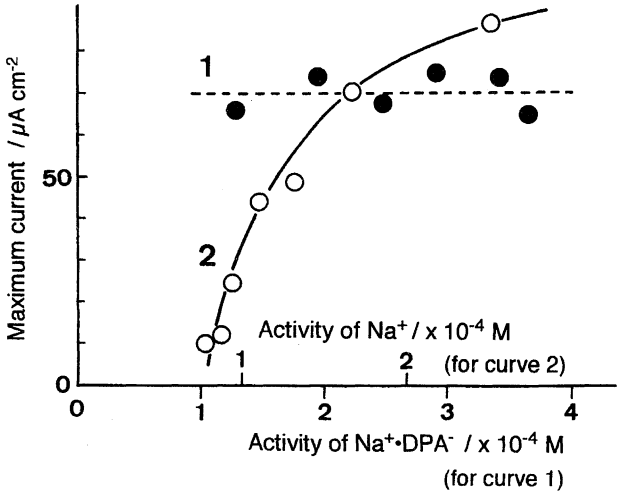

Fig. 6. Dependence of maximum peak currents in voltammograms at the LM/W2 interface on activities of dissociated Na^+ and ion pair, Na^+DPA^-. Curve 1; dependence on the activity of Na^+DPA^- (activity of dissociated $Na^+ = 1.6\times10^{-4}$ M). Curve 2; dependence on the activity of dissociated Na^+ (activity of $Na^+DPA^- = 2.0\times10^{-4}$ M).

mum was practically independent of $a_{Na^+DPA^-}$.

The maximum observed with the transfer of Na^+ at the LM/W2 interface was suppressed completely by the addition of 10^{-6} M BSA into W2 by which the oscillations were also inhibited.

The above-mentioned results on the voltammograms indicate that the condition available for the oscillation of the membrane current or potential resembles closely that for the appearance of the maximum.

5. Drop Time–Potential Curve at the W/NB Interface. The drop time–potential curve at the electrolyte solution dropping electrode is expected to be very useful for the elucidation of the adsorption behavior at an aqueous/organic interface, as described previously.[14,23,24]

Curve 1 in Fig. 7 is the drop time–potential curve investigated using a polarographic cell, and measuring the drop time of W containing 1 M $MgSO_4$ which was forced dropwise into NB containing 4×10^{-4} M Na^+DPA^- and 0.02 M $TPhAs^+DPA^-$. When the curve was compared with that in the absence of Na^+ (Curve 2), there existed a depressed part in the former, suggesting the interfacial adsorption of chemical species relative to Na^+. Assuming that W and NB in the polarographic measurement correspond to W2 and LM, respectively, in the membrane system of Eq. 1, the potential range for the depression resembles that available for both the transfer of Na^+ from LM to W2 and the appearance of the maximum peak at the LM/W2 interface (cf., voltammogram 3 in Fig. 5). Here, the potential range for the depression lies at more positive potentials than the point of zero charge (*pzc*) of the interface at around 0.2 V vs. TPhAsE, and hence W is polarized to be positive in the potential range.

The depression was more conspicuous with an increase of a_{Na^+}, but was practically indifferent to $a_{Na^+DPA^-}$ in the bulk of NB. Taking into consideration both results on the maximum peak current shown in Fig. 6 and the drop time–potential curve mentioned above, it is considered that Na^+ which has been transferred from NB to W may adsorb at the interface from the side of W inducing the adsorption of DPA^- as

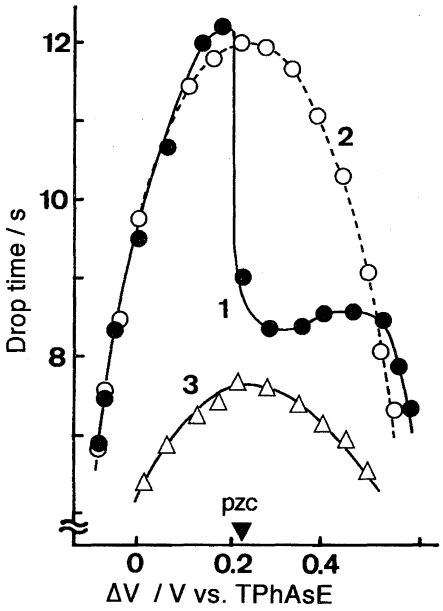

Fig. 7. Drop time–potential curves measured at the W/NB interface. Compositions of W and NB: curve 1; 1 M $MgSO_4$ in W and 4×10^{-4} M Na^+DPA^- +0.02 M $TPhAs^+DPA^-$ in NB, curve 2; as curve 1 but in the absence of Na^+DPA^- in NB, curve 3; as curve 2, but in the presence of 10^{-6} M BSA in W.

a counter ion from the side of NB. At the interface, the adsorbed Na^+ may exist as an ion pair, Na^+DPA^-. In this regards, the possibility of the interfacial ion pair formation between a hydrophobic cation (or anion) in an organic phase and a hydrophilic anion (or cation) in an aqueous phase has been proposed by and Girault and Schiffrin,[25] and Kakiuchi, et al.[26]

6. Mechanisms of the Oscillation. 6.1 Oscillation of Membrane Current under an Applied Membrane Potential. The mechanism will be discussed referring to the voltammograms in Fig. 5.

The oscillation of the membrane current is brought about by the mutually-dependent transfer reactions at the W1/LM and LM/W2 interfaces. When ΔV_{W1-W2} in the range effective for the maximum in curve 1 in Fig. 5 is applied to a membrane system of Eq. 1, $\Delta V_{LM/W2}$ settles at a potential (B) available for both the transfer of Na^+ from LM to W2 and the adsorption of Na^+ as Na^+DPA^- at the LM/W2 interface, and $\Delta V_{W1/LM}$ at a potential (A) in the final descent due to the transfer of Na^+ from W1 to LM. Here, it should be noted that a relation such as Eq. 3 holds among ΔV_{W1-W2}, $\Delta V_{W1/LM}$ and $\Delta V_{LM/W2}$, and magnitudes of currents flowing across the W1/LM and LM/W2 interfaces, $I_{W1/LM}$ and $I_{LM/W2}$, are of the same magnitude (and equivalent to I_{W1-W2}).

At $\Delta V_{LM/W2}$ of B, Na^+ transfers from LM to W2, and the Na^+ transferred to W2 adsorbs at the LM/W2 interface as Na^+DPA^-. The adsorption generates the stirring of the solution in the vicinity of the interface because the adsorption induces the change of the interfacial tension at the LM/W2 interface. Since the stirring enhances the transfer of Na^+ at the interface, $I_{LM/W2}$ grows up as the maximum current. At the same time, $I_{W1/LM}$ grows up along the final descent of the voltammogram at the W1/LM interface (see, curve 2 in Fig. 5), causing the negative shift of $\Delta V_{W1/LM}$ (to A′). The negative shift of $\Delta V_{W1/LM}$ results in the positive shift of $\Delta V_{LM/W2}$ (to B′) because of the relation of Eq. 3. The adsorption at B′ may be stronger than that at the original $\Delta V_{LM/W2}$ (B), since B′ is a potential more remote from *pzc* than B, and hence the polarization of the LM/W2 interface is more significant at B′ than that at B. The duration of the adsorption brings about the saturation of Na^+DPA^- at the interface and the reduction of the stirring. Because of the reduced stirring and the consumption of Na^+ in LM near to the interface owing to the enhanced transfer of Na^+, $I_{LM/W2}$ decreases. Simultaneously, $I_{W1/LM}$ decreases accompanying the positive shift of $\Delta V_{W1/LM}$ to around A and the negative shift of $\Delta V_{LM/W2}$ to around B (cf., Eq. 3). At the $\Delta V_{LM/W2}$ around B where is nearer to *pzc* than B′, Na^+DPA^- which has been adsorbed at the LM/W2 interface desorbs into LM, because the adsorption at this $\Delta V_{LM/W2}$ (around B) is weaker than that at the positive $\Delta V_{LM/W2}$ (B′), and Na^+DPA^- is hydrophobic rather than hydrophilic. The desorption followed by the dissociation of the ion pair restores the activity of Na^+ in LM in the vicinity of the interface. Hence, the current increases again, causing the positive shift of $\Delta V_{LM/W2}$. These processes may repeat to realize the oscillation of the membrane current.

In this regards, the shifts of $\Delta V_{W1/LM}$ and $\Delta_{LM/W2}$ accompanied with the current oscillation were clearly observed, as shown in curves 2 and 3 of Fig. 2.

6.2 Induction or Inhibition of the Current Oscillation. The induction of the oscillation of the membrane current by the addition of Ach^+ can be understood with the aid of ion transfer voltammograms at the W1/LM and LM/W2 interfaces (Fig. 8). In Fig. 8, curves 1 and 2 are schematic illustrations of voltammograms 2 and 3 in Fig. 5, and curve 3 is the voltammogram for the transfer of Ach^+ from W1 to LM.

When −0.30 V is applied as ΔV_{W1-W2} to the cell of Eq. 1 in the absence of Ach^+, $\Delta V_{W1/LM}$ and $\Delta V_{LM/W2}$ settle at potentials indicated as C and D, respectively, and satisfy the relation of Eq. 3. The potential D is not effective for the adsorption of Na^+, and hence for the maximum current. When Ach^+ is added into W1 to be 2×10^{-4} M (cf., curve 3), $\Delta V_{W1/LM}$ shifts to a less negative potential (C′) because the current at the W1/LM interface ($I_{W1/LM}$) is undertaken by the transfer of Ach^+ from W1 to LM. At the same time, according to the relation of Eq. 3, $\Delta V_{LM/W2}$ shifts to a potential (D′) less positive than D, and effective for the adsorption of Na^+ as Na^+DPA^-. At D′, $I_{LM/W2}$ grows up as the maximum current since the transfer of Na^+ from LM to W2 is enhanced by the stirring caused by the adsorption. With the growth of $I_{LM/W2}$, $I_{W1/LM}$ due to the transfer of Na^+ as well as Ach^+ from W1 to LM increases. Some processes similar to those for the oscillation of the membrane current mentioned previously may succeed, and the oscillation induced by Ach^+ may be realized.

The life time of the induced current oscillation is considered to be determined by the concentration of Ach^+, and the oscillation may terminate when the concentration of Ach^+ in W1 is decreased, owing to its transfer from W1 to LM, which explains the result that the life time was shorter with lower concentrations of Ach^+. The higher concentration limit of Ach^+ effective for the induction can be understood by considering as follow. When Ach^+ of concentration higher than 3×10^{-4} M is added to W1, the positive shift of $\Delta V_{W1/LM}$ due to the transfer of Ach^+ is too large and causes a negative

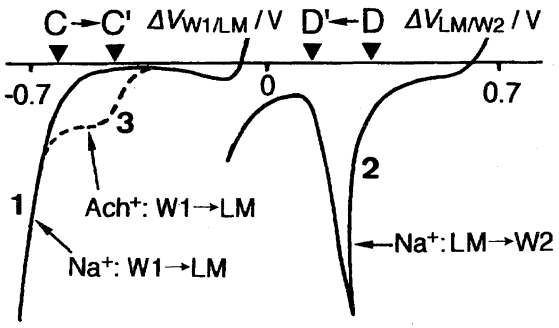

Fig. 8. Voltammetric explanation for the induction of the oscillation by acetylcholine ion (Ach^+) under the applied membrane potential of −0.30 V. Curves 1 and 2; schematic illustration of curves 2 and 3 in Fig. 5. Curve 3; the voltammogram recorded at the W1/LM interface in the presence of 2×10^{-4} M Ach^+ in W1.

shift of $\Delta V_{LM/W2}$ (cf., Eq. 3) to a potential less positive than the range for the maximum current. Therefore, the oscillation cannot be induced when the concentration of Ach^+ is higher than 3×10^{-4} M.

The inhibition of the oscillation by tetraalkylammonium ions can be explained referring to voltammograms in Fig. 9. In the following, the inhibition by 0.01 M TEA^+ will be adopted as an example. Curves 1, 2 and 3 in the figure schematically illustrate voltammograms 1, 2 and 3 in Fig. 5, respectively. Curves 1′ and 2′ are voltammograms observed under the same condition as that for curves 1 and 2, but adding 0.01 M TEA^+ to W1.

Since the final descent in the voltammogram at the W1/LM interface in the presence of 0.01 M TEA^+ in W1 (curve 2′) lies at much more positive potentials than those in the absence of TEA^+ (curve 2), the maximum in the *VITTM* for the transfer of Na^+ in the presence of TEA^+ (curve 1′) appears at more positive potentials than that in the absence of TEA^+ (curve 1) for the sake of the relation of Eq. 3. Therefore, the ΔV_{W1-W2} value necessary to observe the current oscillation in the absence of TEA^+ (e.g., −0.48 V) is too negative to continue the oscillation after the addition of TEA^+.

The inhibition by BSA is attributable to the strong adsorption of BSA on the LM/W2 interface. As clearly seen in the drop time–potential curve (curve 3 in Fig. 7) obtained at the W/NB interface by using a polarographic cell, the drop time of an aqueous solution containing 10^{-6} M BSA and 1 M $MgSO_4$ was quite short over a wide potential range, indicating that BSA adsorbs on the W/NB interface in the potential range on both side of *pzc* as pointed out by Vanýsec and Sun.[27] Because the interface is occupied by the adsorbed BSA, and hence Na^+ cannot adsorb there, the current oscillation does not appear. In this connection, the adsorption of BSA is supposed to be fairly slow, since the significant depression in the drop time–potential curve was observed only when the drop time of W was quite long like that in the experiment of Fig. 7.

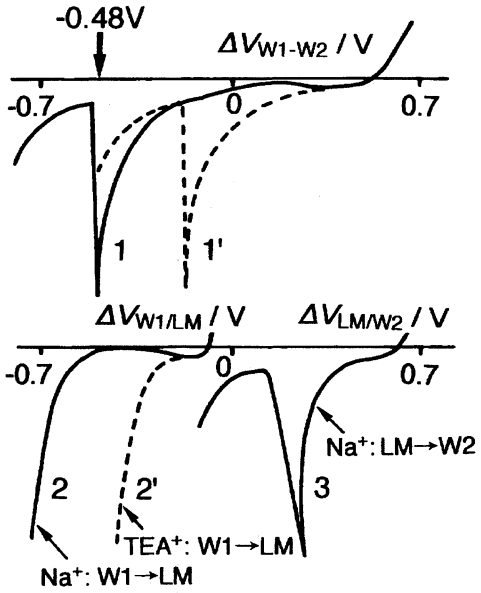

Fig. 9. Voltammetric explanation for the inhibition of the oscillation by TEA^+. Curves 1, 2, and 3; schematic illustration of curves 1, 2, and 3 in Fig. 5. Curves 1′ and 2′; voltammograms recorded under the same condition for curves 1 and 2, but in the presence of 0.01 M TEA^+ in W1.

6.3 Oscillation of Membrane Potential under an Applied Membrane Current. The mechanism will be discussed with the aid of Fig. 10. Curve 1 schematically illustrates the voltammogram at the LM/W2 interface observed with the cell of Eq. 1 (curve 3 in Fig. 5), and curve 2 or 3 is the voltammogram for the transfer of TBA^+ or $TPrA^+$ from LM containing 0.02 M TBA^+DPA^- or $TPrA^+DPA^-$ to W2, respectively.

When I_{W1-W2} available for the transfer of cations from W1 to W2 is applied to the membrane system of Eq. 1, Na^+ transfers at the LM/W2 interface, since the transfer free energy of Na^+ from NB to W is much smaller than that of $TPhAs^+$. The Na^+ transferred to W2 adsorbs at the LM/W2 interface as Na^+DPA^-, and the adsorption generates the stirring of solutions in the vicinity of the interface. The stirring enhances the ion transfer at the interface resulting in a current maximum which is much larger than the ordinary current due to the ion transfer being controlled by the diffusion. Hence, when the I_{W1-W2} larger than the diffusion-controlled current but smaller than the maximum current is applied, $\Delta V_{LM/W2}$ is settled at a potential in the region where the maximum appears (e.g., E in Fig. 10 when $I_{W1-W2}=-20$ $\mu A\,cm^{-2}$). Here, it should be noted that the $\Delta V_{LM/W2}$ is more positive than *pzc* of the W/NB interface at around 0.2 V vs. TPhAsE. Due to the enhanced transfer of Na^+ at the $\Delta V_{LM/W2}$, the concentration of Na^+ in LM near to the interface decreases more extensively than that in the case of the diffusion-controlled ion transfer.

The adsorption continues during the transfer of Na^+, although the change of the interfacial tension caused by the adsorption of Na^+ becomes smaller and the stirring becomes weaker when an appropriate amount of Na^+DPA^- is ac-

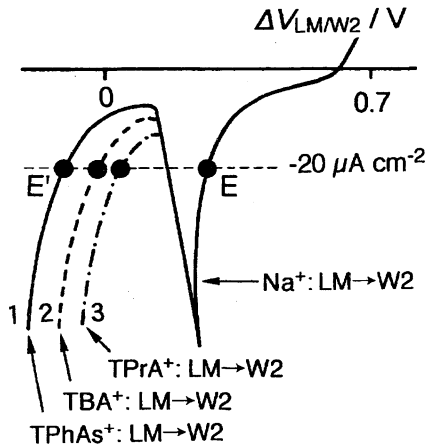

Fig. 10. Voltammetric explanation for the potential oscillation. Curve 1; schematic illustration of curve 3 in Fig. 5. Curves 2 and 3; voltammograms recorded at the LM/W2 interface employing TBA^+DPA^- and $TPrA^+DPA^-$ as supporting electrolyte in LM instead of $TPhAs^+DPA^-$.

cumulated, and the LM/W2 interface approaches the state saturated with Na^+DPA^-. As the results of the consumption of Na^+ and the weakened stirring, the flux of Na^+ to the interface from the bulk of LM decreases to be too small to undertake the applied I_{W1-W2}. Then, the coexisting SE cation, $TPhAs^+$, which requires more energy to transfer at the interface than Na^+ may participate in carrying a part of the applied I_{W1-W2}. At this time, $\Delta V_{LM/W2}$ shifts to a potential more negative (E′ in Fig. 10) than the original (E). At E′ where is more negative than *pzc*, Na^+DPA^- which has been adsorbed desorbs from the interface toward LM, as expected from the drop time-potential curve in Fig. 7. Owing to the desorption and the dissociation of the desorbed Na^+DPA^-, the concentration of Na^+ in LM near to the interface may be restored to be enough to carry the applied I_{W1-W2}. At this time, $\Delta V_{LM/W2}$ returns to E, where the adsorption of Na^+ occurs. These processes are then repeated to realize the oscillation of $\Delta V_{LM/W2}$. The oscillation of $\Delta V_{LM/W2}$ causes the oscillation of ΔV_{W1-W2} since Eq. 3 holds among ΔV_{W1-W2}, $\Delta V_{W1/LM}$, and $\Delta V_{LM/W2}$. Here, $\Delta V_{W1/LM}$ is kept almost constant during the oscillation because the applied I_{W1-W2} at the W1/LM interface is carried by the transfer of Na^+, which exists in W1 in high concentration.

It is obvious from the discussion above that the amplitude of the potential oscillation is determined by transfer potentials (which correspond to transfer free energies) of two ions (Na^+ and $TPhAs^+$ in the present case) transferring at the oscillating interface. Therefore, the difference in amplitude of the potential oscillations observed with different SE cations such as $TPhAs^+$, TBA^+, or $TPrA^+$ can be understood by consulting Fig. 10, and taking into account the transfer potentials of SE cations.

7. Relation between the Oscillations and Voltammetric Maxima. Various NB-membrane systems other than Eq. 1, such as Eq. 4 to Eq. 16, have also been investigated in our laboratory in order to elucidate the general features of the oscillations of membrane current or potential.

[W1]	[LM; NB]		
0.1 M KCl 1 M $MgSO_4$ (SE)	4×10^{-4} M K^+DPA^-, 0.02 M $TPhAs^+DPA^-$ (SE)	[W2] 2 M $MgSO_4$(SE)	(4)
0.1 M CsCl 1 M $MgSO_4$ (SE)	4×10^{-4} M Cs^+TPhB^-, 0.05 M $THexA^+TPhB^-$ (SE)	2 M $MgSO_4$ (SE)	(5)
0.1 M TMA^+Cl^- 1 M $MgSO_4$ (SE)	4×10^{-4} M TMA^+TPhB^-, 0.05 M $THexA^+TPhB^-$ (SE)	2 M $MgSO_4$ (SE)	(6)
0.1 M NaI 1 M $MgSO_4$ (SE)	5×10^{-4} M $THexA^+I^-$, 0.05 M $THexA^+TPhB^-$ (SE)	2 M $MgSO_4$ (SE)	(7)
0.1 M NaBr 1 M $MgSO_4$ (SE)	5×10^{-4} M $THexA^+Br^-$, 0.05 M $THexA^+TPhB^-$ (SE)	2 M $MgSO_4$ (SE)	(8)
1 M $MgSO_4$ (SE)	0.05 M $THexA^+TPhB^-$ (SE)	2.5×10^{-4}M$(TPenA^+)_2SO_4^{2-}$ 2 M $MgSO_4$ (SE)	(9)
1 M $MgSO_4$ (SE)	0.05 M $THexA^+TPhB^-$ (SE)	5×10^{-4}M Na^+Pic^- 2 M $MgSO_4$ (SE)	(10)
0.1 M Na^+Pic^- 1 M $MgSO_4$ (SE)	5×10^{-4} M $THexA^+Pic^-$ 0.05 M $THexA^+TPhB^-$ (SE)	2 M $MgSO_4$ (SE)	(11)
1 M $MgSO_4$ (SE)	0.05 M $THexA^+TPhB^-$ (SE)	5×10^{-4} M TMA^+Cl^- 2 M $MgSO_4$ (SE)	(12)
1 M $MgSO_4$ (SE)	0.05 M $THexA^+TPhB^-$ (SE)	5×10^{-4} M $NaClO_4$ 2 M $MgSO_4$ (SE)	(13)
1 M $MgSO_4$ (SE)	0.05 M $THexA^+TPhB^-$ (SE)	5×10^{-4} M NaBr 2 M $MgSO_4$ (SE)	(14)
0.01 M $TPrA^+Cl^-$ 1 M $MgSO_4$ (SE)	5×10^{-4} M $TPrA^+TPhB^-$ 0.05 M $THexA^+TPhB^-$ (SE)	2 M $MgSO_4$ (SE)	(15)
1 M $MgSO_4$ (SE)	0.05 M $THexA^+TPhB^-$ (SE)	5×10^{-4} M $TPenA^+Br^-$ 2 M $MgBr_2$ (SE)	(16)

The I_{W1-W2} or ΔV_{W1-W2} applied were those effective for ion transfer reactions, as follows. K^+ from W1 to W2 (Eq. 4),

Cs^+ from W1 to W2 (Eq. 5), TMA^+ from W1 to W2 (Eq. 6), I^- from W1 to W2 (Eq. 7), Br^- from W1 to W2 (Eq. 8), $TPenA^+$ from W2 to LM, and $THexA^+$ from LM to W1 (Eq. 9), Pic^- from W2 to LM, and $TPhB^-$ from LM to W1 (Eq. 10), Pic^- from W1 to W2 (Eq. 11), TMA^+ from W2 to LM and $THexA^+$ from LM to W1 (Eq. 12), ClO_4^- from W2 to LM and $TPhB^-$ from LM to W1 (Eq. 13), Br^- from W2 to LM and $TPhB^-$ from LM to W1 (Eq. 14), $TPrA^+$ from W1 to W2 (Eq. 15) and $TPenA^+$ from W2 to LM and $THexA^+$ from LM to W1 (Eq. 16).

It has been found that oscillations of I_{W1-W2} or ΔV_{W1-W2} could be realized by employing membrane systems of Eq. 4 to Eq. 10, although further experiments are required to describe the details of the oscillations. When membrane systems such as Eq. 11 to Eq. 16 were examined, however, the oscillations were not observed at any I_{W1-W2} or ΔV_{W1-W2}. The oscillations of ΔV_{W1-W2} observed were confirmed to be due to the oscillations of the potential difference at the LM/W2 interface, $\Delta V_{LM/W2}$.

Since the voltammetric maximum due to the adsorption was essential for the appearance of the oscillations of I_{W1-W2} or ΔV_{W1-W2} observed with the membrane system of Eq. 1, voltammograms (polarograms) were investigated by using a polarographic cell and employing W and NB of which the compositions were the same as those of W2 and LM, respectively, in cells of Eq. 4 to Eq. 16 (but concentrations of $MgSO_4$ or $MgBr_2$ in W were 1 M instead of 2 M).

Polarograms observed are illustrated in Fig. 11. Though potential differences in the measurements were applied as potentials of a silver/silver chloride electrode in W vs. TPhAsE or TPhBE in NB, they were converted into the TPhE scale according to the previous paper,[17,18] and plotted as the abscissa in Fig. 11. The *pzc* at the interface lies at around 0 V vs. TPhE, which means the transfer free energy is zero.

It is obvious from Figs. 5 and 11 that following polarographic waves are accompanied by a maximum; (a) the negative current wave for the transfer of such a hydrophilic cation as Na^+, K^+, Cs^+ or TMA^+ from NB to W which appears in the potential range more positive than *pzc*, (b) the positive current wave for the transfer of such a hydrophilic anion as I^- or Br^- from NB to W which appears in the potential range less positive than *pzc*, (c) the positive current wave for the transfer of such a hydrophobic cation as $TPenA^+$ from W to NB which appears in the potential range less positive than *pzc*, and (d) the negative current wave for the transfer of such a hydrophobic anion as Pic^- from W to NB which appears in the potential range more positive than *pzc*. However, the following polarographic waves are not accompanied by a maximum; (e) the negative current wave for the transfer of such a hydrophobic cation as $TPrA^+$ from NB to W which appears in the potential range less positive than *pzc*, (f) the positive current wave for the transfer of such a hydrophobic anion as Pic^- from NB to W which appears in the potential range more positive than *pzc*, (g) the positive current wave for the transfer of such a hydrophilic cation as TMA^+ from W to NB which appears in the potential range more positive than *pzc*, and (h) the negative current wave for the transfer of such a hydrophilic anion as ClO_4^- or Br^- from W to NB which appears in the potential range less positive than *pzc*.

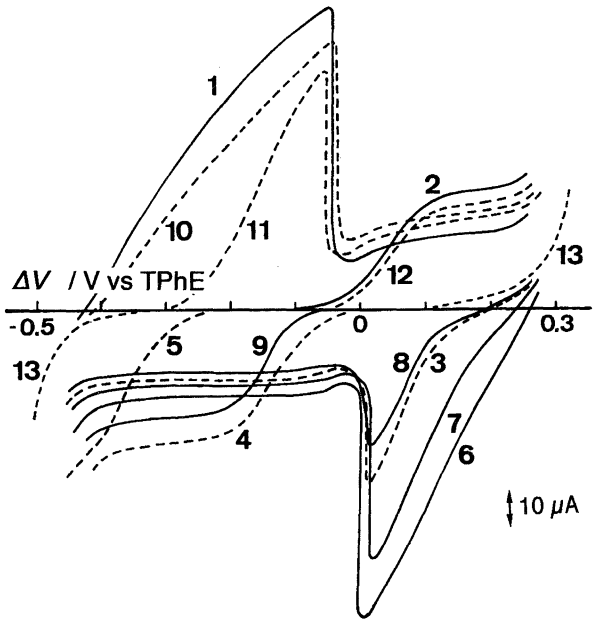

Fig. 11. Polarograms for transfers of various ions at the W/NB interface. Concentration of objective ion in W or NB; 5×10^{-4} M. Supporting electrolytes; 1 M $MgSO_4$ in W and 0.05 M $THexA^+TPhB^-$ in NB. Curve 1, 2, 3, 4 or 5; transfer of $TPenA^+$, TMA^+, Pic^-, ClO_4^- or Br^-, respectively, from W to NB. Curve 6, 7, 8, 9, 10, 11 or 12; transfer of K^+, Cs^+, TMA^+, $TPrA^+$, Br^-, I^-, or Pic^-, respectively, from NB to W. Curve 13; residual current.

Drop time–potential curves were investigated under the same conditions as those for the polarographic measurements; it was confirmed that all polarographic maxima observed were caused by adsorptions of transferring ions at W/NB interface.

Comparing the results on the oscillations with those on the polarographic maxima, it was found that the voltammetric maximum due to the adsorption of the transferring ion at one of two LM/W interface is the requisite for the oscillations of membrane current or membrane potential. However, the oscillations were not observed with the membrane system of Eq. 16, though they were observed with the membrane system of Eq. 9, and the transfer of $TPenA^+$ from W to NB gave a polarographic maximum. Such results suggest that the condition available for the oscillations is not necessarily the same as that for the voltammetric maximum.

As described concerning the oscillation mechanisms, the recovery of the concentration of the objective ion in the interfacial region of one phase from which the ion transfers to another is necessary in order to get the sustained oscillations. The recovery is attained by the dissociation of the desorbed ion pair which has been accumulated at the interface. In the case of the membrane system of Eq. 9, $TPenA^+$ transferred from W2 to LM adsorbs at the interface from the side of LM, inducing the adsorption of SO_4^{2-} as a counter ion from the side of W2, and exists as the ion pair, $(TPenA^+)_2SO_4^{2-}$, at the interface. Since $(TPenA^+)_2SO_4^{2-}$ is composed of

very hydrophilic SO_4^{2-}, it is considered to be rather hydrophilic, so $(TPenA^+)_2SO_4^{2-}$ may desorb into W2. On the other hand, in the case of the membrane system of Eq. 16, transferred $TPenA^+$ adsorbs at the LM/W2 interface from the side of LM inducing the adsorption of Br^- from the side of W2, and exists as $TPenA^+Br^-$ at the interface. Since $TPenA^+Br^-$ is composed of Br^- which is much less hydrophilic than SO_4^{2-}, it is considered to be rather hydrophobic, so $TPenA^+Br^-$ may desorb into LM. Therefore, the concentration of $TPenA^+$ in W2 near the interface can be recovered by the desorption, followed by the dissociation in the case of Eq. 9, but cannot be recovered in the case of the Eq. 16. This consideration suggests that the direction of the desorption of the ion pair is another important factor to get the oscillations.

Conclusion

In the present paper, novel oscillations of membrane current or potential accompanied by the transport of Na^+ through a liquid membrane have been introduced, and it has been stressed that the characteristics of the current oscillation were somewhat similar to those of the oscillations at a biomembrane with a "sodium channel" from the viewpoint of the induction and inhibition. The usefulness of the voltammetric methods and concepts in the elucidation of mechanisms of membrane oscillations has also been emphasized.

The voltammetric methods and concept are expected to be applicable also to the analysis of the oscillation at a very thin membrane such as a *BLM*, since even the ion transfer through a *BLM* can be observed as a voltammogram and interpreted by the way similar to that for a liquid membrane.[20,21]

Though the ion transfer was realized by applying a definite membrane potential or membrane current in the examples of oscillations introduced in the present paper, the authors assume that the consideration presented here may be available for the interpretation of the oscillation accompanied by the transfer of an ion promoted by the transfer of the other ions[28,29] or by an interfacial redox reaction, i.e., electron transfer, if the role of the transfer of the other ions or the electron transfer could be regarded as that of the applied potential or current.[30,31]

This work was partly supported by a Grant-in-Aid for Scientific Research No. 07454200 from the Ministry of Education, Science, Sports and Culture.

References

1) G. J. Siegel, "Basic Neurochemistry," Raven Press, New York (1989).
2) R. Larter, *Chem. Rev.*, **90**, 355 (1990).
3) S. Kihara and K. Maeda, *Prog. Surf. Sci.*, **47**, 1 (1994).
4) K. Yoshikawa, M. Shoji, S. Nakata, and S. Maeda, *Langmuir*, **4**, 759 (1988).
5) Y. Miyazaki, K. Hayashi, K. Toko, K. Yamafuji, and N. Nakayama, *Jpn. J. Appl. Phys.*, **31**, 1555 (1992).
6) B. Sakmann and E. Neher, "Single-Channel Recording," Plenum Press, New York (1983).
7) C. Miller, "Ion Channel Reconstitution," Plenum Press, New York (1986).
8) S. Numa, *Harvey Lec.*, **83**, 121 (1989).
9) S. Kihara, K. Maeda, O. Shirai, Y. Yoshida, and M. Matsui, in "Bioelectroanaysis, 2," ed by E. Pungor, Akadémiai Kiadó, Budapest (1993), p. 331.
10) J. Koryta, *Electrochim. Acta*, **29**, 445 (1984).
11) H. H. J. Girault and D. J. Schiffrin, in "Electroanalytical Chemistry," "Vol. 15: Electrochemistry of Liquid–Liquid Interface," ed by A. J. Bard, Marcel Dekker, New York (1989), p. 1.
12) M. Senda, T. Kakiuchi, and T. Osakai, *Electrochim. Acta*, **36**, 253 (1991).
13) A. Volkov and D. W. Deamer, "Liquid–Liquid Interfaces. Theory and Methods," CRC Press, Boca Raton (1996).
14) K. Maeda, S. Kihara, M. Suzuki, and M. Matsui, *J. Electroanal. Chem.*, **295**, 183 (1990).
15) S. Kihara, K. Maeda, O. Shirai, M. Suzuki, K. Ogura, and M. Matsui, *Bunseki Kagaku*, **40**, 767 (1991).
16) S. Kihara, Z. Yoshida, and T. Fujinaga, *Bunseki Kagaku*, **31**, E297 (1982).
17) S. Kihara, M. Suzuki, K. Maeda, K. Ogura, S. Umetani, M. Matsui, and Z. Yoshida, *Anal. Chem.*, **58**, 2954 (1986).
18) S. Kihara, M. Suzuki, K. Maeda, K. Ogura, and M. Matsui, *J. Electroanal. Chem.*, **210**, 147 (1986).
19) S. Kihara, M. Suzuki, M. Sugiyama, and M. Matsui, *J. Electroanal. Chem.*, **249**, 109 (1988).
20) O. Shirai, S. Kihara, Y. Yoshida, and M. Matsui, *J. Electroanal. Chem.*, **389**, 61 (1995).
21) O. Shirai, S. Kihara, Y. Yoshida, K. Maeda, and M. Matsui, *Bull. Chem. Soc. Jpn.*, **69**, 3151 (1996).
22) T. Shedlovsky and R. L. Kay, *J. Phys. Chem.*, **60**, 151 (1956).
23) T. Kakiuchi, M. Kobayashi, and M. Senda, *Bull. Chem. Soc. Jpn.*, **60**, 3109 (1987).
24) Z. Yoshida and S. Kihara, *J. Electroanal. Chem.*, **227**, 171 (1987).
25) H. H. J. Girault and D. J. Schiffrin, *J. Electroanal. Chem.*, **170**, 127 (1984).
26) T. Kakiuchi, M. Kobayashi, and M. Senda, *Bull. Chem. Soc. Jpn.*, **61**, 1545 (1988).
27) P. Vanysek and P. Sun, *Bioelectrochem. Bioenerg.*, **23**, 177 (1990).
28) M. Dupeyrat and E. Nakache, *Bioelectrochem. Bioenerg.*, **5**, 134 (1978).
29) K. Yoshikawa and Y. Matsubara, *Biophys. Chem.*, **17**, 183 (1983).
30) K. Maeda, S. Kihara, M. Suzuki, and M. Matsui, *J. Electroanal. Chem.*, **303**, 171 (1991).
31) H. Ohde, K. Maeda, O. Shirai, Y. Yoshida, and S. Kihara, *J. Electroanal. Chem.*, in press.